

Head and Neck

Evaluation of the accuracy of computer-assisted techniques in the interstitial brachytherapy of the deep regions of the head and neck

Guo-Hao Zhang^{1,6}, Xiao-Ming Lv^{1,6}, Wen-Jie Wu¹, Zhi-Yuan Wu¹, Lei Zheng¹,
Ming-Wei Huang¹, Yong Wang², Jian-Guo Zhang^{1,*}

¹Department of Oral and Maxillofacial Surgery, Peking University School and Hospital of Stomatology, Haidian District, Beijing, PR China

²Center of Digital Dentistry, Peking University School and Hospital of Stomatology, National Engineering Laboratory for Digital and Material Technology of Stomatology, Research Center of Engineering and Technology for Digital Dentistry, Ministry of Health, Beijing Key Laboratory of Digital Stomatology, Haidian District, Beijing, PR China

ABSTRACT

PURPOSE: We sought to investigate the feasibility and accuracy of computer-assisted techniques in the interstitial brachytherapy of the deep regions of the head and neck.

MATERIALS AND METHODS: A computer-assisted brachytherapy workflow was applied to 10 patients with tumors in the deep regions of the head and neck. Based on the brachytherapy treatment preplan, we constructed a digital stereotactic model to accurately transfer the virtual plan into the navigation system, and subsequently printed the individual templates. The navigation system and the individual template were combined together to visualize and guide brachytherapy needle implantation. Preoperative and intraoperative image data were reconstructed and registered to measure and analyze the needle deviation.

RESULTS: A total of 58 needles were successfully inserted in 10 patients with the guidance of computer-assisted techniques and a mean deviation of 5.2 mm. The inserting trajectories and depths of the needles were as follows: from the parotid and masseter regions to the infratemporal fossa or skull base, the range was 15.7–74.6 mm; from the submandibular and retromandibular regions to the infratemporal fossa or skull base, the range was 15.6–70.6 mm; from the infraorbital region to the pterygomandibular region, the range was 63.7–69.7 mm; and from the periorbital region to the intraorbital region, the range was 47.6–61.8 mm. The dose distribution met the treatment requirement well.

CONCLUSIONS: The computer-assisted interstitial brachytherapy workflow was proven to be feasible and accurate for the deep regions of the head and neck. © 2018 American Brachytherapy Society. Published by Elsevier Inc. All rights reserved.

Keywords:

Computer-assisted technique; Individual template; Navigation; Brachytherapy; Accuracy; Head; Neck

Introduction

Permanent interstitial brachytherapy has been cumulatively used and has resulted in good outcomes for primary or adjuvant treatment of prostate cancer, gynecologic malignancies, and certain head and neck tumors (1–7). By means of radioactive sources (usually ¹²⁵I, ¹⁹²Ir, or ¹⁰³Pd), which are implanted into the target area via percutaneous needles, the treatment can deliver high doses of radiation into the tumor mass while sparing the adjacent normal tissues (8–10), an ability that is especially beneficial for the treatment of tumors in the deep regions of the head and neck (9–11).

To ensure that radiation doses cover the target area while also minimizing side effects, brachytherapy needle trajectories and seed distribution locations are preplanned

Received 29 June 2018; received in revised form 14 November 2018; accepted 6 December 2018.

The related study was presented as an oral presentation at the 2018 American Brachytherapy Society Annual Meeting in San Francisco, CA, USA.

Financial disclosure: The authors report no proprietary or commercial interests in any products mentioned or concepts discussed in this article.

Funding source: This research did not receive any specific grant from funding agencies in the public, commercial, or not-for-profit sectors.

* Corresponding author. Department of Oral and Maxillofacial Surgery, Peking University School and Hospital of Stomatology, No. 22 Zhongguancun South Avenue, Haidian District, Beijing 100081, PR China. Tel.: 86-010-82195242; fax: 86-010-82195701.

E-mail address: rszhang@126.com (J.-G. Zhang).

⁶ Guo-Hao Zhang and Xiao-Ming Lv are joint first authors and they contributed equally to this work.

according to the tumor sites and the surrounding anatomical structures in the brachytherapy treatment planning system (BTPS) before operation. As radioactive sources are implanted via percutaneous needles, the success of brachytherapy depends largely on the precise placement of these needles. Nevertheless, it is extremely difficult to perform brachytherapy if the target area locates in the deep regions of the head and neck. First, the application of brachytherapy in deeper anatomic regions may cause adverse events because of mechanical injuries or prompt radiation damage to adjacent critical organs and tissues (e.g., carotid artery, jugular vein, eyes, bones, nerves). Second, the complex bony structures, including the maxilla, mandible, zygomatic arch, and sphenoid bone, obstruct needle implantation into the deep regions of the head and neck and may eventually impact dose distribution (12). Moreover, the paranasal sinuses in the craniofacial bone limit the placement of radioactive seeds to a degree. Therefore, it is vital to accurately transfer the optimized virtual preplan to the implantation procedure to provide effective and precise brachytherapy in these regions. Even though the needle-insertion procedure can be image-guided [for example, by way of ultrasound (13), computed tomography (CT) (14), or magnetic resonance imaging (15, 16)] or template-guided (17–19), the application of brachytherapy to the deep regions of the head and neck is generally technically challenging to surgeons and oncologists.

However, with the rapid and ongoing development of novel methods, computer-assisted techniques are becoming widely used and have obtained satisfactory outcomes in head and neck surgery (20–23). The techniques consist of virtual surgical simulation, computer-aided design/computer-aided manufacture, rapid prototyping, reverse engineering, and surgical navigation. However, only a few reports have been published at this time on the subject of the entire workflow of computer-assisted techniques for interstitial brachytherapy of the deep regions of the head and neck. To provide intraoperative visualization of the preplanned needle trajectories and the real-time needle positions to improve needle-insertion accuracy, a preplanned interstitial brachytherapy workflow assisted by digital techniques has been established in our institute, applying both individual template guidance and infrared navigation system guidance. In this clinical study, we report on the application results of the workflow in 10 patients, with the purpose of determining the feasibility and accuracy of the process in the deep regions of the head and neck.

Methods and materials

Patients

Ten patients with histologically proven, locally advanced, or recurrent head and neck tumors were included in the present study. After informed consent was obtained,

the individuals were treated according to the computer-assisted brachytherapy workflow (Fig. 1) at the Peking University School and Hospital of Stomatology in Beijing, China. Initially, patients underwent medical history review and completed physical and radiological examinations. They were reviewed by surgical colleagues and deemed unsuitable for salvage surgery. The tumors involved skull base, infratemporal fossa, pterygoid fossa, deep lobe of the parotid gland, and parapharyngeal space. The histologic types included rhabdomyosarcoma (five cases), adenoid cystic carcinoma (two cases), desmoid-type fibromatosis (one case), mucoepidermoid carcinoma (one case), and primitive neuroectodermal tumor (one case). The present study was approved by the ethics committee of the Peking University School and Hospital of Stomatology.

Workflow

Brachytherapy treatment planning

Before implantation, a contrast-enhanced CT scan was acquired for each patient. Data presented in the Digital Imaging and Communications in Medicine (DICOM) format were imported into a BTPS (Beijing Astro Technology Ltd Co., Beijing, China) to generate a brachytherapy treatment plan. The planned target volume was defined as gross tumor volume and its surrounding potential subclinical lesions or microscopic lesions. Based on the key factors of that the determined dose was optimally delivered to the target area, and that normal tissues were minimally injured, the entrance and end point and orientation of the needle trajectories as well as the distribution of ^{125}I radioactive seeds

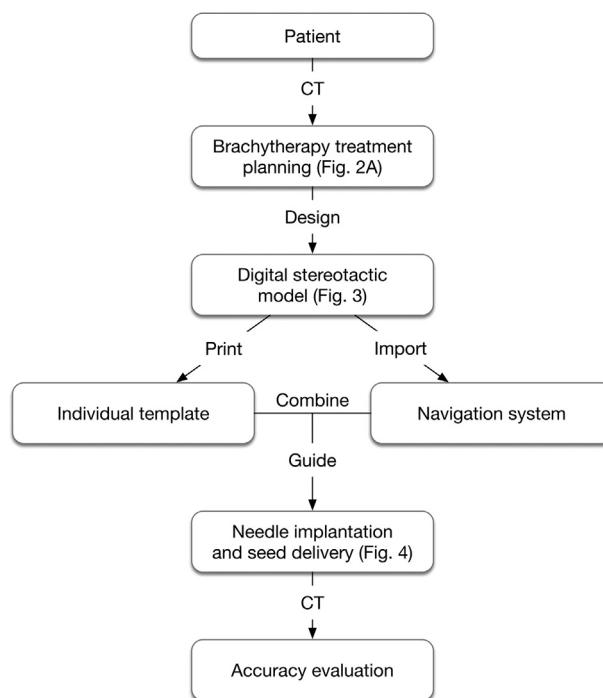


Fig. 1. Overview of the computer-assisted brachytherapy workflow.

were planned. The activity of ^{125}I radioactive seeds (model 6711, Beijing Atom and High Technique Industries Inc., Beijing, China) ranged from 0.5 mCi to 0.7 mCi. Specifically, high-risk needle trajectories (e.g., the trajectory that was adjacent to the carotid artery in Fig. 2a) were finely adjusted and defined as key needle trajectories. The position data of the needle trajectories were exported.

Computer-assisted preoperative preparation

The CT data were imported into Mimics software (version 10.01; Materialise, Leuven, Belgium) to reconstruct the three-dimensional (3D) appearance of the skin in the head and neck region. Following this, reverse engineering, by way of the Geomagic Studio 2012 (3D Systems, Morrisville, NC, USA), was used to read the 3D skin appearance data in standard triangulation language format and the position data of the needle trajectories. Then, the digital model of the individual template was designed and printed through a rapid prototyping technique, which was detailed in a previously published study (19, 24). Notably, the individual template contains the information of skin contour, and the cylinders on it can guide

needle insertion according to the preplan. On the basis of the digital individual template model, digital models of the key needle trajectories were constructed according to the position data. The digital model of one needle trajectory was made up of a right circular cone object and a cylinder object. The coordinates of virtual midpoint of the deepest seed in a needle trajectory were used to create the apex of cone object, and the axis of cone object and cylinder object was set according to the coordinates of the virtual needle trajectory. Between five and seven digital needle trajectory models were constructed in one case and were added to the digital individual template model with application of a Boolean operation to obtain the final digital model (Fig. 3), which was defined as the digital stereotactic model (DSM). Then, the DSM in standard triangulation language format and the patient's CT data in DICOM format were imported into the iPlan CMF 3.0 software (BrainLAB, Feldkirchen, Germany) to create the navigation plan. The needle trajectories were marked according to DSM, and the apices of the cone objects were set as targets. The carotid artery and jugular vein were additionally marked according to CT data (Fig. 2b).

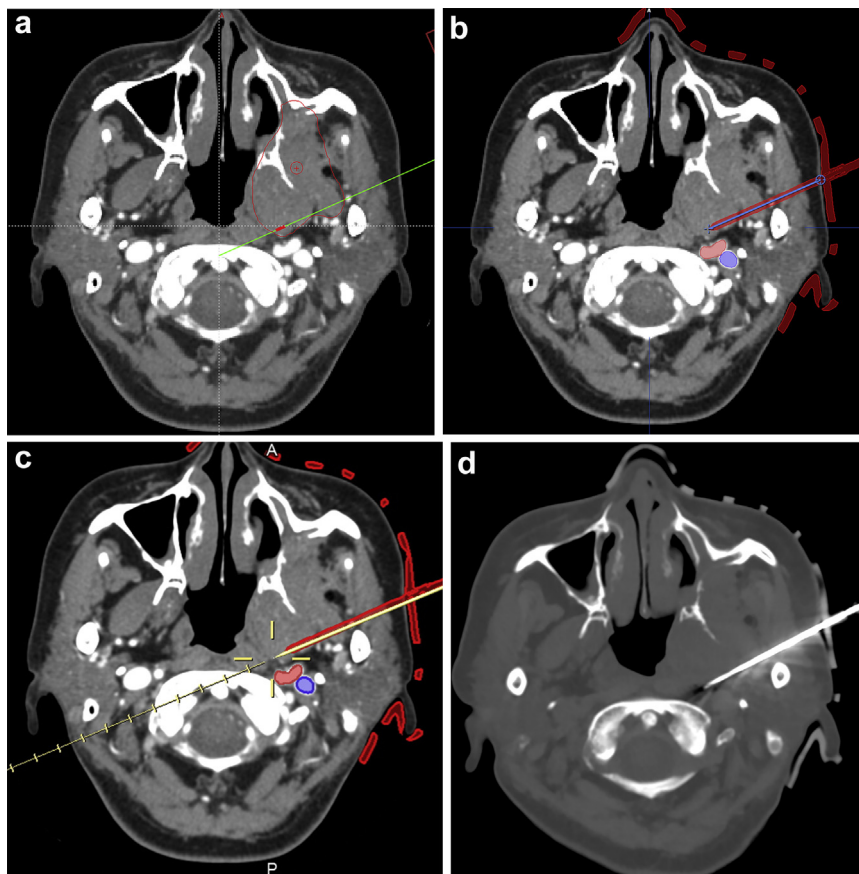


Fig. 2. Needle implantation from preplan to implementation in the deep regions of the head and neck: (a) The preplanned needle-insertion trajectory and depth in brachytherapy treatment planning system. The red target on the green line represented the end point of the implantation. (b) The digital stereotactic model and CT data were imported into iPlan CMF software to create the navigation plan. The needle-insertion trajectory (blue line), carotid artery, and jugular vein were marked. (c) Intraoperative image-guided needle insertion (yellow line). (d) A CT scan was performed after needle insertion to verify the actual position of the needle. (For interpretation of the references to color in this figure legend, the reader is referred to the Web version of this article.)

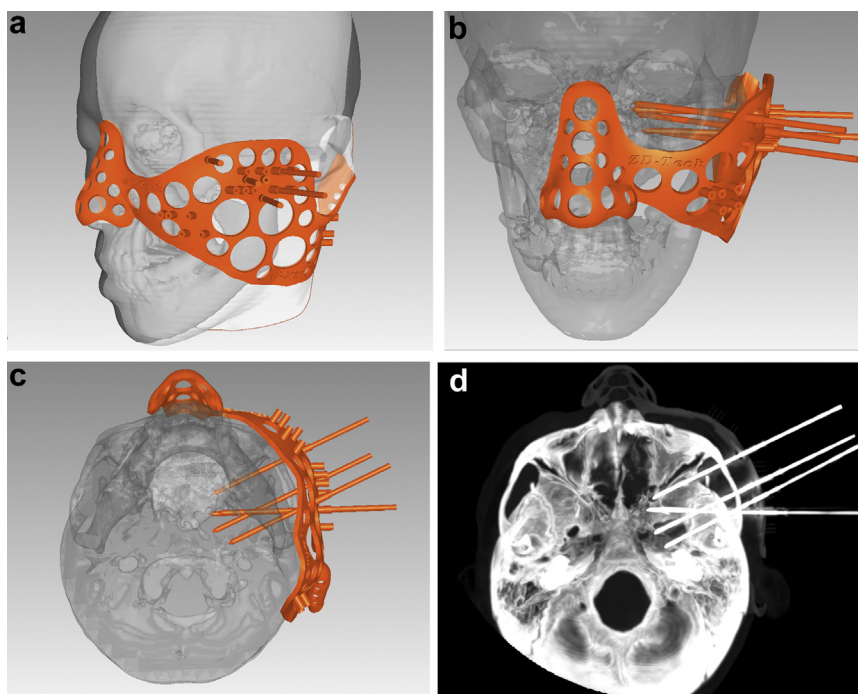


Fig. 3. The appearance of digital stereotactic model on three-quarter view (a), anterior view (b), and inferior view (c). The actual position of needles and individual template were in accordance with digital stereotactic model (d).

Navigation system preparation

Before surgery, the navigation system (BrainLAB, Feldkirchen, Germany) was set up in the CT room. The navigation system consists of the computer platform with a screen and the localization system. The localizer is composed of two optical cameras, which emit infrared light and receive reflective light to detect the location of the reflective marker spheres in real time. The reflective marker spheres are mounted on the reference frame, which is fixed on patient's head, the surgical probe, and the percutaneous needle. Under general anesthesia, the patient was placed on the CT bed. After the navigation registration process, the patient's actual head position was correlated to the virtual head position in the navigation system. Moreover, DSM that contained the position information of the individual template and needle trajectories, CT data of the patient, the surgical probe, and the percutaneous needle were displayed in real time on the screen of the computer platform (Fig. 2c).

Needle implantation and seed delivery

Initially, the individual template was put into position in three steps: first, it was placed on the patient's facial area according to the skin contour; second, the position of the individual template was finely adjusted under the assistance of the navigation system, confirming that the actual position of the individual template was in line with the virtual plan; and third, the operator implanted three needles with shallow depths in the margin area of the individual template to immobilize the template. The final location of the individual template was thereafter verified by intraoperative

CT. Afterward, the needles in key needle trajectories were implanted with guidance of the preplanned virtual needle trajectories on the screen of the navigation computer platform and the cylinders on the individual template (Fig. 4). The inserting orientation was adjusted in real time according to the virtual trajectory in the navigation system, and the implantation was deemed completed when the needle reached the target on platform screen (Fig. 2c). A CT scan was performed when all of the targets were reached to evaluate and adjust the actual needle positions (Figs. 2d and 3d). After completion of the needle insertion according to the key needle trajectories, the remaining needles were inserted with the guidance of cylinders on the



Fig. 4. The needles were implanted with the guidance of the individual template and the navigation system.

individual template. Next, ^{125}I seeds were delivered via the needles according to the preplan, and CT scans were acquired for intraoperative dose distribution verification. The general anesthesia ended after verification of the dose distribution.

Accuracy evaluation

Needle position error

To evaluate the accuracy of needle implantation, the DICOM format files from the preoperative CT scan and intraoperative CT scan were imported into the Mimics software. Based on segmentation technology, we reconstructed the preoperative craniofacial bone. The preplanned digital needle trajectory models were added to the craniofacial bone model while applying Boolean operation in Geomagic software, which made up the preoperative model. Subsequently, we reconstructed the intraoperative CT to obtain the intraoperative model, which consisted of the intraoperative craniofacial bone model and the placed needle models. Applying a “best-fit registration function”, the preoperative and intraoperative models were registered according to the periorbital and frontal regions of the bone (considered as the fixed anatomical structure). Therefore, the preplanned needle trajectories and the intraoperative placed needles were rigidly transformed into the same coordinate frame for comparison. Specifically, the needle deviation was measured in terms of the needle tip position, namely the distance from the apex of the cone object in the preoperative needle trajectory model to the tip of the intraoperatively placed needle model. The actual insertion depth from the entrance point on the skin surface to the needle tip was measured using the CT data.

Postoperative verification

Based on intraoperative CT data obtained following ^{125}I seeds delivery, the dose distribution was evaluated. The D_{90} (dose delivered to 90% of the target volume), V_{100} (the percentage of the target volume receiving at least 100% of the planned dose), and V_{150} (the percentage of the target volume receiving at least 150% of the planned dose) were calculated in the BTPS.

Statistical analysis

Statistical analysis was carried out using the SPSS version 13.0 for Windows software (SPSS Inc., Chicago, IL, USA). The Pearson correlation coefficient was used to analyze the correlation between the needle distance deviation and the actual insertion depth. A two-sided p value of < 0.05 was considered to be statistically significant.

Results

For all the 10 patients, computer-assisted interstitial brachytherapy was feasible in the deep regions of the head

and neck. Intraoperative real-time visualization and guidance of needle implantation were accomplished. The operator implanted the needles following the digital workflow, and the radioactive seeds were delivered as planned. The average procedure time was 120.2 minutes for each patient from the beginning of setting up the navigation system to the end of general anesthesia, during which the preparation time of the digital workflow was approximately 30 minutes, and the mean needle implantation time (from individual template placement to the point of all needle implantations being accomplished) was 41.7 minutes. As a result, there was no adverse effect reported in any of the 10 patients.

A total of 58 needles were inserted in key needle trajectories. The mean needle distance deviation was 5.2 mm for each needle, and needle deviations ranged from 1.3 mm to 13.2 mm (Table 1). The needle-insertion trajectories and depths were as follows: from the parotid and masseter region to the infratemporal fossa or skull base, the range was 15.7–74.6 mm; from the submandibular and retromandibular region to the infratemporal fossa or skull base, the range was 15.6–70.6 mm; from the infraorbital region to the pterygomandibular region, the range was 63.7–69.7 mm; and from the periorbital region to the intraorbital region, the range was 47.6–61.8 mm. The correlation between needle distance deviation and the actual insertion depth was nonsignificant at a 0.05 level.

As for dose distribution, the mean D_{90} was $105.3 \text{ Gy} \pm 16.8 \text{ Gy}$ (range: 79.4–131.0 Gy), and it was larger than the planned dose in all patients. In addition, the V_{100} was larger than 90% and the V_{150} was less than 50% in all patients.

Discussion

Brachytherapy can deliver high and conformal radiation doses to the target area and ensure minimal trauma is caused to adjacent normal tissues, which in particular has

Table 1

The tumor sites, the number of needles in key needle trajectories, and the distance deviation in terms of the needle tip

No.	Localization	No. of needles	Deviation (mm)		
			Mean	Range	SD
1	Skull base	6	5.0	2.5–6.5	1.7
2	Skull base	5	2.6	1.5–3.5	0.8
3	Parapharyngeal space	6	4.0	1.3–6.0	1.7
4	Skull base	6	6.1	5.1–7.4	0.9
5	Skull base	6	4.4	2.4–6.8	1.5
6	Deep lobe of parotid gland	5	7.0	1.8–12.8	4.3
7	Pterygoid fossa	7	5.4	4.1–7.3	1.2
8	Skull base	5	4.3	2.7–7.1	1.8
9	Infratemporal fossa	6	6.7	4.5–9.9	1.9
10	Infratemporal fossa	6	5.9	2.6–13.2	4.1

SD = standard deviation.

Mean indicates mean deviation of all the needles in key needle trajectories of each case, and range indicates the range of deviation, from the minimal deviation to the maximum deviation of each case.

advantages in the treatment of tumors in the deep regions of the head and neck (9–11). Before operation, it is beneficial to create a precise plan in a BTPS, which gives oncologists enough time to optimize the needle trajectories and seed distribution locations (5–7,9,19,25). Nevertheless, an ideal virtual plan in a BTPS does not necessarily imply the precise execution of the plan. In deep regions of the head and neck, brachytherapy has to be performed under general anesthesia, so it is vital to insert needles in the desired position(s) during a one-time procedure. If not, the time of anesthesia must be prolonged or even another operation must be performed under anesthesia to correct seed distribution, significantly increasing the risk of complications. To accurately transfer a virtual plan into a clinical procedure, a computer-assisted workflow has been established, whose preliminary results have demonstrated that the workflow was clinically feasible. The deviation was measured regarding the planned versus placed needle tips, and the mean deviation was 5.2 mm for 58 needles of the 10 patients.

As far as we know, a very limited number of reports have been published to date regarding the evaluation of accuracy of brachytherapy guidance (8,19,26–28). In the literature, the mean needle deviation ranged from 1 mm to 15 mm in various body regions. Among them, Bale *et al.* reported three cases with tumors involving deep regions of the head and neck (the skull base), where brachytherapy was performed with the guidance of a frameless stereotactic navigation system (8). The approximate mean needle deviation of the three cases reported was 2 mm, 3 mm, and 13 mm, respectively. In our study of 10 patients, the deviation was measured precisely through image reconstruction and registration. The mean distance deviation of the planned and placed need tips was 5.2 mm. Considering the long insertion depth and complex surrounding anatomy, the workflow was proven to be accurate even without fixing the head. Various factors may influence the accuracy of needle insertion. Notably, phantom studies reported that the targeting error of the needle was positively correlated with the insertion depth (11, 29). However, in our study, the correlation of the needle distance deviation and the actual insertion depth was nonsignificant at a 0.05 level, which may be attributed to our limited sample size. Furthermore, because of the research methods used, we can hardly estimate the uncertainties in each part of the process respectively, such as deviation of navigation registration, deviation of template placement, anatomic change, needle deflection, and so on. However, in this study, the D_{90} , V_{100} , and V_{150} met the treatment requirements well, indicating that the distance deviation of needle implantation is acceptable for the individual cases included, with no relevant compromise of target coverage.

From our institute, Huang *et al.* published the application of a 3D-printed individual template for needle guidance in head and neck brachytherapy (19, 24). The individual template consists not only of the information

of a patient's skin surface appearance, which is used to assist placement, but also of the data of the needle entrance point and inserting orientation, making needle implantation a quick, accurate, and single-attempt procedure. In the computer-assisted workflow, the infrared navigation system and 3D-printed individual template are combined together to visualize and guide needle implantation. In one trajectory, the deepest ^{125}I seed is delivered first and then the needle is retracted 1–1.5 cm each time to deliver the remaining ^{125}I seeds sequentially, according to the preplan. Thus, the virtual midpoint of the deepest seed in the BTPS is set as the target point of needle insertion. As virtual planning data are incompatible between the BTPS and the iPlan CMF software, the DSM serves as a “bridge” to accurately transfer the virtual planning data from the BTPS to the iPlan CMF software.

The computer-assisted brachytherapy workflow has certain advantages. For example, with the planned and actual needle trajectories displayed simultaneously on the screen, the operator can compare and correct needle deviation during implantation, and the use of the individual template can avoid sources of human error. Furthermore, in a single case, multiple needle trajectories can be designed and needles can be guided to be inserted in different orientations without moving position of the head. Besides, all the needle trajectories are preplanned and prepared for intraoperative guidance, making the operation of needle implantation a one-time and easy procedure, which shortens the operation time and reduces adverse reactions. Moreover, even though the navigation system and individual template do not allow real-time monitoring of soft tissue mobility and displacement during needle insertion, the intraoperative CT imaging provides authentic feedback and allows for real-time verification and adjustment of the needle position. Last but not least, with the distributions of radioactive seeds and radiation doses accurately preplanned and implemented, the target area is covered with a lesser number of seeds.

Nevertheless, the use of a computer-assisted workflow does have some disadvantages: as the procedure of preparation is based on the preoperative CT data, alterations in the volume and the shape of tumor or organ between the time of the preplan and the needle implantation may lead to inaccurate outcomes as well as prolonged time in registration and guidance procedures. Also, owing to facial soft tissue deformation, the placement of the individual template was not stable in the first few implantations of needles. In addition, the preparation time of the workflow is longer as compared with the regular procedure. Therefore, a subsequent study will focus on the development of an updated workflow, in which the brachytherapy treatment plan and the computer-assisted preparation will be based on intraoperative CT data. The individual template will additionally be designed to cover hard tissues (e.g., teeth) to limit movement. Moreover, even though the additional preparation time is beneficial to the patient and can improve the overall

outcomes, the working team will be trained to become more skillful and the operation procedures will be arranged in a more connected fashion to shorten the preparation time.

Conclusions

The computer-assisted interstitial brachytherapy workflow employed in the present study was proven to be feasible and accurate in deep regions of the head and neck. A 3D individual template and an infrared navigation system were successfully combined together to precisely provide a virtual treatment plan in the operation and guidance of needle insertion.

References

- [1] Morris WJ, Tyldesley S, Rodda S, et al. Androgen suppression combined with elective nodal and dose escalated radiation therapy (the ASCENDE-RT trial): an analysis of survival endpoints for a randomized trial comparing a low-dose-rate brachytherapy boost to a dose-escalated external beam boost for high- and intermediate-risk prostate cancer. *Int J Radiat Oncol Biol Phys* 2017;98:275–285.
- [2] Sturdza A, Pötter R, Fokdal LU, et al. Image guided brachytherapy in locally advanced cervical cancer: improved pelvic control and survival in RetroEMBRACE, a multicenter cohort study. *Radiother Oncol* 2016;120:428–433.
- [3] Takacsi-Nagy Z, Martinez-Mongue R, Mazon JJ, et al. American brachytherapy society task group report: combined external beam irradiation and interstitial brachytherapy for base of tongue tumors and other head and neck sites in the era of new technologies. *Brachytherapy* 2017;16:44–58.
- [4] Wierzbicka M, Bartochowska A, Strnad V, et al. The role of brachytherapy in the treatment of squamous cell carcinoma of the head and neck. *Eur Arch Otorhinolaryngol* 2016;273:269–276.
- [5] Wu WJ, Shao X, Huang MW, et al. Postoperative iodine-125 interstitial brachytherapy for the early stages of minor salivary gland carcinomas of the lip and buccal mucosa with positive or close margins. *Head Neck* 2017;39:572–577.
- [6] Huang MW, Wu WJ, Lv XM, et al. The role of (125I) interstitial brachytherapy for inoperable parotid gland carcinoma. *Brachytherapy* 2018;17:244–249.
- [7] Mao MH, Zheng L, Wang XM, et al. Surgery combined with postoperative (125I) seed brachytherapy for the treatment of mucoepidermoid carcinoma of the parotid gland in pediatric patients. *Pediatr Blood Cancer* 2017;64:57–63.
- [8] Bale RJ, Freysinger W, Gunkel AR, et al. Head and neck tumors: fractionated frameless stereotactic interstitial brachytherapy-initial experience. *Radiology* 2000;214:591–595.
- [9] Huang MW, Zheng L, Liu SM, et al. 125I brachytherapy alone for recurrent or locally advanced adenoid cystic carcinoma of the oral and maxillofacial region. *Strahlenther Onkol* 2013;189:502–507.
- [10] Pappas IP, Ryan P, Cossmann P, et al. Improved targeting device and computer navigation for accurate placement of brachytherapy needles. *Med Phys* 2005;32:1796–1801.
- [11] Zhu JH, Wang J, Wang YG, et al. Prospect of robotic assistance for fully automated brachytherapy seed placement into skull base: Experimental validation in phantom and cadaver. *Radiother Oncol* 2017; <https://doi.org/10.1016/j.radonc.2017.11.031>.
- [12] Das RK, Keleti D, Zhu Y, et al. Validation of monte carlo dose calculations near 125I sources in the presence of bounded heterogeneities. *Int J Radiat Oncol Biol Phys* 1997;38:843–853.
- [13] Davis BJ, Horwitz EM, Lee WR, et al. American brachytherapy society consensus guidelines for transrectal ultrasound-guided permanent prostate brachytherapy. *Brachytherapy* 2012;11:6–19.
- [14] Lee LJ, Damato AL, Viswanathan AN. Clinical outcomes of high-dose-rate interstitial gynecologic brachytherapy using real-time CT guidance. *Brachytherapy* 2013;12:303–310.
- [15] de Arcos J, Schmidt EJ, Wang W, et al. Prospective clinical implementation of a novel magnetic resonance tracking device for real-time brachytherapy catheter positioning. *Int J Radiat Oncol Biol Phys* 2017;99:618–626.
- [16] Menard C, Susil RC, Choyke P, et al. MRI-guided HDR prostate brachytherapy in standard 1.5T scanner. *Int J Radiat Oncol Biol Phys* 2004;59:1414–1423.
- [17] Paley PJ, Koh WJ, Stelzer KJ, et al. A new technique for performing syed template interstitial implants for anterior vaginal tumors using an open retropubic approach. *Gynecol Oncol* 1999;73:121–125.
- [18] Lindegaard JC, Madsen ML, Traberg A, et al. Individualised 3D printed vaginal template for MRI guided brachytherapy in locally advanced cervical cancer. *Radiother Oncol* 2016;118:173–175.
- [19] Huang MW, Zhang JG, Zheng L, et al. Accuracy evaluation of a 3D-printed individual template for needle guidance in head and neck brachytherapy. *J Radiat Res* 2016;57:662–667.
- [20] Zheng L, Lv X, Zhang J, et al. Translating computer-aided design and surgical planning into successful mandibular reconstruction using a vascularized iliac-crest flap. *J Oral Maxillofac Surg* 2018;76:886–893.
- [21] Gong X, He Y, An J, et al. Application of a computer-assisted navigation system (CANS) in the delayed treatment of zygomatic fractures: a randomized controlled trial. *J Oral Maxillofac Surg* 2017; 75:1450–1463.
- [22] Monaco C, Ragazzini N, Scheda L, et al. A fully digital approach to replicate functional and aesthetic parameters in implant-supported full-arch rehabilitation. *J Prosthodont Res* 2018;62:383–385.
- [23] Yu Y, Zhang WB, Liu XJ, et al. A new procedure assisted by digital techniques for secondary mandibular reconstruction with free fibula flap. *J Craniofac Surg* 2016;27:2009–2014.
- [24] Huang MW, Liu SM, Zheng L, et al. A digital model individual template and CT-guided 125I seed implants for malignant tumors of the head and neck. *J Radiat Res* 2012;53:973–977.
- [25] Liu SM, Wang HB, Sun Y, et al. The efficacy of iodine-125 permanent brachytherapy versus intensity-modulated radiation for inoperable salivary gland malignancies: study protocol of a randomised controlled trial. *BMC Cancer* 2016;16:193.
- [26] Strassmann G, Heyd R, Cabillie-Engenhart R, et al. Accuracy of 3-d needle navigation in interstitial brachytherapy in various body regions. *Strahlenther Onkol* 2002;178:644–647. discussion 648–649; author reply 650.
- [27] Krempien RC, Grehn C, Haag C, et al. Feasibility report for retreatment of locally recurrent head-and-neck cancers by combined brachy-chemotherapy using frameless image-guided 3D interstitial brachytherapy. *Brachytherapy* 2005;4:154–162.
- [28] Krempien R, Hoppe H, Kahrs L, et al. Projector-based augmented reality for intuitive intraoperative guidance in image-guided 3D interstitial brachytherapy. *Int J Radiat Oncol Biol Phys* 2008;70:944–952.
- [29] Wan G, Wei Z, Gardi L, et al. Brachytherapy needle deflection evaluation and correction. *Med Phys* 2005;32:902–909.